Effect of K2O/ZnO+CaO Ratio on Density, Glass Forming Ability, Crystallization of SiO2- Al2O3- ZnO- K2O- CaO Frites

aida faghinia (aida.faeghinia@gmail.com)
Materials and Energy Research Center
R. Salami
Materials and Energy Research Center
Z. Khakpour
Materials and Energy Research Center
M. Zakeri
Materials and Energy Research Center

Research Article

Keywords: Glaze, ZnO, size, frites, TEC

Posted Date: May 11th, 2021

DOI: https://doi.org/10.21203/rs.3.rs-500765/v1

Abstract

The frites by mole fraction of 2.5 SiO_2, 0.20 Al_2O_3, 0.15 B_2O_3, 0.15ZnO, 0.17K_2O, 0.67CaO systems in three ratios of S including 0.37(denoted by F1frites),0.31(F2), 0.24(F3) (S=K_2O/CaO+ZnO) were studied. ZnO powder with 500 nm (N series) and >1μm sizes (F series) opted from the recycled Zn ingots dusts and commercially ZnO respectively, were used as the raw materials.

By decreasing the S ratio, the Molar Volumes of frites were decreased, The glass transition ΔT_g(=-154ºC), and the crystallization temperatures ΔT_p (=+17ºC) values were decreased and increased respectively. It was shown that the GS (glass stability) values are independent of the Zinc Oxide's powder size, while the Molar Volumes of N series were lower than the F ones.

The Zinc Silicate (Willemite) beside Anorthite and Parawollastonite phases were crystallized in the resulted glazes. The hardness values were in 700-850 Hv range, the transparency and whiteness were higher than 80 and 60 respectively.

1. Introduction

It is well known that, Zinc oxide, ZnO, is an environmentally friendly and technically important semi-conductor [1]. Due to a unique combination of electrical and optical properties, it is one of the most attractive semiconductors. Besides this, its potential applications are catalysis, optoelectronic devices, sensors and photovoltaic devices. ZnO can be synthesized in a wide range of particle sizes and shapes [2]. ZnO-CaO-Al_2O_3-SiO_2 system used in industry to produce transparent and glossy glazes [3].

In the case of ZnO application for glaze, It was shown that [3], in the smaller quantities, ZnO acts as a flux. It works especially strongly in the glazes with the high contents of SiO_2 and Al_2O_3. It enhances the gloss of the glazes and improves the performance of opaque glazes. However, this compound is expensive and many attempts have been done before, to change the glaze's formulation in a way that the ZnO amount decreased [4, 5, 6]. In the recent research [4], it was shown that the glaze rich in ZnO would be crystallized in the calcium silicate form. This phase formation could be avoided by the alumina addition in 2 to 4 wt. %. In addition, the alumina source in this study supplied from kaolinite increases the resulted glaze transparency. In other research [5] it was shown that by blending two transparent and opal frites, the ZnO content decreased to 0.5 wt.% but the density and crystalline phases of this frites were not discussed at all. In other work [6], it was shown that zircon in substitution of zinc oxide improves the mechanical properties of the glaze but they demonstrated that the zinc oxide plays an important role in the whiteness controlling. Moreover, their experiments showed that the whiteness (up to 85.7%) and flexural strength (47.61 MPa) at the maximal content of zircon (14.5 wt. %) and a low content of ZnO (2.5 wt. %) were accomplished.

Willemite (Zn_2SiO_4) - gahnite ($ZnAl_2O_4$) are the main crystalline phases of ZnO-CaO-Al_2O_3-SiO_2 glazes, which formed with different morphologies. The kinetics of the seed's formation and the growth of

willemite and gahnite crystals in such materials have been widely reported [7]. Willemite crystals exhibit different morphologies, varying with the melt's viscosity, which that is depended on the glaze composition , the crystal growth temperature, and on the cooling rate of heat treatment [8].

On the other hand, Nanometric particles were developed in the typical glaze systems for innovative surface characteristics in floor and wall tile industries [9]. So imparting of the nano particle technology adheres a greater attention to the ceramic products via yielding outstanding properties [10]. The use of ZnO nanoparticles (NPs) has generated serious concern about their fate, transportation, and toxicity in the environment. ZnO in glaze industry supposed as a modifier that could be dissolved faster than the alkaline oxide and decreased the glass viscosity around the T_g temperature [11]. It has been demonstrated, that the major effects in the melting kinetics and the major variations in reaction paths are directly attribute to the particle size distributions of the batch components [12]. In this work, the fine size sample was generated by upgrading of Halid bearing Zinc Oxide concentrate from the recycling of Zn ingots dusts [13].

However, the mixed effect of alkaline oxides and ZnO was not investigated. Therefore, in this attempt, the focus was on the ZnO compound with two different sizes (sources) through the different K_2O/CaO+ZnO ratios, to determine how will ZnO particle sizes distribution influence on glass melting, frites density, and final color of the glazes. The frites characters (crystallization and Molar Volume) and the resulted glazes were studied.

Several transparent frit formulations containing synthetic and commercial available ZnO powders in varying amounts were prepared under laboratory conditions. Physical properties of the 500-nano and a micrometer ZnO powder containing glazes (including density, glass forming ability, crystalline phases, glass stability, FT-IR, hardness and colors) were compared.

2. Experimental Procedure

Fine ZnO powder was generated at the laboratory scale by a sustainable and environmentally friendly process of upgrading of HZO (Halide bearing Zinc Oxide) concentrate. First, chemical, mineralogical and physical properties of this Nano -ZnO and a standard ZnO provided commercially were measured. Then, six frit compositions containing different ZnO powders by varies S=K_2O/CaO+ZnO ratios were prepared under laboratory conditions. The composition in wt. % of the frites, were chosen from reference[14], as these types of glasses are very sensitive to phase separation, the selected compositions were chosen from the center of compositional triangle proposed by [14] to avoid the opal appearance (Fig.1).

The frites composition were 2.5 SiO_2, 0.20 Al_2O_3, 0.15 B_2O_3, (0.15+x) ZnO, (0.17+y) K_2O, (0.67-z) CaO (in mole fraction). The raw materials of the frites were, (K_2CO_3 Merck, Art No. 7734, Germany), $CaCO_3$ (Merck, Art No. 5828, Germany), Al2O3 (Merck, Art No. 5550, Germany), B_2O_3 (Merck, Art No 7783 Germany), ZnO (CAS Number, 13 463) and pure optical grade silica (Azandarian Mining Company, Iran).

The S values were varied in 0.37, 0.31, 0.24 relations and the resulted frites were denoted by the F1, F2, F3, respectively as shown in the Table1.

Batches mixed in an agate mortar, and were melted in a platinum crucible at the temperature range of 1450-1550 °C. The melts were held for 2 hrs. and then quenched in cooled water. The obtained frites were grinded using fast milling, screened by 400 mesh sieves and the resulted frites were mixed with different additive to prepare the slurry with 1.5 g/cm^3 density. Table 2 shows the wt. % of the additives to make the slurry. Formerly the slurries were sprayed on the fired commercial wall tile. Firing were carried out at 1070 ºC-1160ºC for 3 minutes [15]. The total firing time was 90 minutes.

The heat treatments were done in a tubular furnace. DTA analysis was performed on the 60 mg frites powder heated at 10°C/min up to 1200°C in a platinum crucible in air (model Netch Germany). Al_2O_3 was used as the reference material. The inflexion point of the endothermic drift on the DTA curve is reported as Tg [9]. XRD analysis were performed using an (PHILIPSPW3710) advanced diffraction system with a Cu Kα radiation (l.5404 Å).Dilatometer softening point (Td) and CTE was also measured by dilatometer (model Netzsch 402E Germany).The microhardness of the samples were measured by indentation technique using Vickers indenter (model MVK-H21). The measurement was done by applying a 100 g load for 15 s. It was taken the average of 10 measurements. Before measurements, the sample surface was polished with 3 µm alumina powder to get

good reactive surface. Scanning electron microscopy (SEM) JEOLJXA-840 was used in order to observe the microstructure and EDX analysis. Samples were mounted onto the sample holder, they were polished and etched then were coated with gold, and then studied with SEM.

L*a*b* color parameters of colored glazes were measured for an illuminant D65, following the CIE-L*a*b* colorimetric method recommended by the CIE (Commission Internationale del'Eclairage). In this system, L* is the degree of lightness and darkness of the color in relation to the scale extending from white (L*=100) to black (L*=0). a* is the scale extending from green (-a*) to red (+a*) axis and b* is the scale extending from blue (-b*) to yellow (+b*) axis.

Fig. 2 shows the XRD patterns of the commercial and nano –synthesized ZnO . It is obvious that the resulted synthetic Nano-ZnO is pure and the peaks are wide.

In order to compare the C_p values of the used ZnO powder, as the raw materials and to compare the melting behavior of the batches, the C_p values of different ZnO powders were measured by DSC, and were presented in Fig.3.

As expected, the synthesized powder at high temperature than 600ºC has at least 0.4 Jg/ºC lower value comparing to the commercial one. This event could led to different thermal properties of obtained glaze, which will be discussed flowingly.

The particle size analysis of the two studied powder and morphologies were evaluated but considering to the agglomeration event in Nano sized powder by Malvern analysis, the exact size of nano powder was not confirmed, but however give us the image of particle size distribution. Figs. 4 shows the PSA of the used powders.

However, it can be said that the synthesized ZnO powder has narrow PSA, and more than 40 vol. % of the used synthesized powder is smaller than 1 micron .

Molar volume calculations2.1.

The molecular weights of the frites were also calculated as described and using these molecular weights and density, the molar volumes of the frites can be calculated from following expression:

$$V_m = \frac{M}{\rho} \quad (1)$$

Here, V_m is molar volume, ρ is the density of the sample and M is the molecular weight of the sample. Helium Pycnometry measured the frites density.

3. Results

3.1. Melting of frites

The XRD patterns of the obtained frites were presented in Fig.5.

The obtained densities, the melting temperatures of six series of the frites with two different ZnO powder size and the calculated values of molar mass and (Coefficient of Thermal Expansion) CTEs were presented in Table 3.

It can be seen that by the increasing of the S ratio (from 0.24 to 0.37) the melting temperatures values of frites were decreased (from 1550 to 1450°C respectively). In frites, CaO and K_2O normally function as network modifiers (ZnO could be has two roles intermediate or modifier) and induce a decrease of the T_m [15].

The variation of molar volumes and S ratios with respect to the ZnO particle sizes (PSA) as a raw material used in frites batches were presented in Fig.6.

The Thermal Expansion Coefficient (CTE) values with various S ratios can be predicted using Appen's equation as follows [16]

$$f = \Sigma f_i p_i \quad (2)$$

Where p_i is the mole fraction of individual oxides and f_i is a characteristic factor for each oxide. f_i for ZnO is 5.0×10^{-6}, B_2O_3 is -5.0×10^{-6}, SiO_2 is 3.8×10^{-6}, Al_2O_3 is -3.0×10^{-6}, CaO is 13.0×10^{-6} and K_2O is 42.0×10^{-6}/K. It can be seen that by decreasing the S ratio, the CTE values of the frites decreased from 6.28×10^{-6}/K to 6.96×10^{-6}/K. In order to compare the resulted CTE of the obtained glazes and the tile's body, the expansion of the used substrate Tile was measured in Fig. 7.

The difference of thermal expansions of the two different tile and glaze compositions linked to each other gives rise to stress in these materials.

3.2. The DTA results

The thermal analysis of the obtained frites were compared as well in Fig.8 and Table 4. The Tg values of frites were not observed sharply and they were recorded in broad temperature range. Also, the crystallization peaks of the samples were not sharp corresponded to the surface crystallization. (However by differentiating of the heat flow graph the onset of T_g were obtained)

The compositions (N1-F1, N2-F2, N3-F3) were the same but the characteristic temperatures were altered (the melting temperatures were changed as well).

The variation of characteristic temperatures T_p, T_g, T_p-T_g by the S ratio with two different ZnO sizes were presented in Figs. 8.

The higher the value of glass transition temperature of a frit, the greater the stability of its elastic properties [17,18]. In order to compare the glass stability of the frites with different ZnO particles sizes and S ratios, the T_P /T_m and T_p -T_g/T_m values vs. frit compounds were represented in Fig.8c and Fig.8d.

This figure shows that the stability of the frites increases as the network modifier contents increase.

FT-IR Evaluation

In Fig.9, the infrared absorption spectra of the experimental frites with different compositions are shown. The absorbance of the spectra were compared to the values given in the literature [19,20,21]. In spectrums, the IR bands are identified as follows: the Si-O(s) stretching mode is located in the range 10000-1200 cm^{-1}, the Si-O (b) bending mode is found around $800cm^{-1}$. Band at 650 cm^{-1} is assigned to the symmetric stretching vibration of Si-O- (Si, Al) between the tetrahedral in N3 and F2 samples.

As the alkali oxide (K_2O) content increased (in F1 sample), the position of the maximum absorbance of the Si-O(s) band shifts towards lower values, until $1044cm^{-1}$.

3.4. Sintering of resulted glazes

Series of sintering conditions at slow and high cooling as well as heating rates were done on F, N glazes that were applied on the fired tile. Keeping the firing temperatures in such a way that the surface of the

glazes would not be phase separated, colored changed or warped by the naked eye. The firing temperatures were increased up to 1180ºC, to obtain the gloss appearance on glazes surfaces.

The heat treatments conditions used and the resulted glaze's appearance were shown in Table 5.

By decreasing the heating rates, the diffusivity increases in the frit and it will promote phase separation. On the other hand, the fast heating rate (90 minutes heating time) led to the higher crystallization temperature, compared to the slow heating rates (150 minutes).

On the other hand, fast heating rates (60 mins, heating.) led to warping of glazed samples due to the thermal gradient in samples. This damage occurs mainly during the cooling, because the bisque tend to shrinks after the fast expanding that may not well-matched with the glaze's shrinkage.

3.5 Phase Evaluation

Fig. 10 shows the phase evaluations of heat treated F2 , F1 and F3 frites at 1000ºC -30 min. in 90 minutes heating time .

The low crystallinity (low peak's intensity) of F1 sample was seen in Fig.10. In F3 sample, (with higher T_{rg} values) the relative intensities of characteristic XRD peaks of wollastonite phase were 3 orders higher than the F1 one.

The phase's evaluations of the resulted sintered glazes at 1060ºC (3 min holding time and 90 minutes heating) on the tile's body were presented in Fig.11..

The Wollastonite phase remains in the F1 sample by the temperature ($\Delta T=+60$), but in the case of F2, F3 samples the crystalline phases (Wollastonite) change to the Calcium Aluminum Silicate(Anorthite)phase which could be related to the low glass stability(GS) of these system. Calcium Aluminum Silicate (Anorthite) was confirmed by the Si-O-Al vibrations at 650 cm^{-1} by the FT-IR results in F2,F3 samples.

The Calcium Silicate and Wollastonite phases remained in N1, F1 and N3 samples by increasing the temperature but the Anorthite phase was appeared in F3 sample.

The XRD peak's intensities (and hence the crystallization ability) were higher in F2 and N2 samples compared to the other sample.

Although F1, N1 compositions have more ZnO content in composition, but the Willemite (Zinc Silicate) phase was not detected in F1, N1,F3,N3 systems, whereas the Zinc Silicate phase was developed in F2 glaze. It can be related to the ZnO_4 unites formation which was demonstrated by FT-IR located at 566.82 cm^{-1} wavelength.

3.6 Micro hardness

The resulted Vickers micro hardness values, crystalline phases of the glazes are also compared in Table 6.

3.7 Optical Properties

The CIE Lab parameters gloss values of the F1 to F3 glazes are given in Table 7. As can be seen, The F1 and F2 glazes present the high gloss values but the F3,N3 glazes show the low GU values corresponded to the higher calcium silicate crystallization [22]. Also the a* value in F1 sample describe the light red color in the glaze. Since the mentioned glazes had been applied onto the Tile without using an engobe layer , utilizing a suitable engobe would enhance their whiteness.

L values and traces amounts of a and b reveal the tendency of both glass ceramic glazes to the white color. The whiteness index of both were obtained around 65%.

3.8 Microstructural Evaluation

The etched and polished surfaces of the samples were presented in Figs.12. All samples show the prismatic morphology which is the characteristic form of pyroxene minerals (Parawollastonite, Anorthite, Calcium Silicate). These crystalline phases have 7.3×10^{-6}/K,4.9×10^{-6}/K,5.4×10^{-6}/K Thermal Expansion Coefficients,(CTE) respectively. The lower CTE of these crystals led to the micro cracks formation around the crystalline phases in samples.

The needle like crystals of Willemites could be observed in F2 and N2 samples as well.

By comparing the XRD peak's intensities and the SEM micrographs of the F1 and N1 samples in Fig.12b it is clear that the crystalline volumes are lower than the N3,N2,N1 sample's .Likewise the F3 sample has almost the smaller prismatic like crystals than the N3 and N2 samples. The micrographs by high magnification are presented in Fig12 b.

The relict morphology of Wollastonite in F1, N2, samples are clearly observed but the F3 and N3 samples shows rounded morphology that could be related to Anorthite and Parawollastonite respectively [23].

Discussion

In this work, it was shown that, although the ZnO amount in F1 sample was higher than F3 but the K_2O role as modifier is responsible for the decreasing of the melting temperature. This means that K_2O can breaks up the network more effectively than ZnO and CaO, respectively. K_2O has a lower IFS than ZnO, and CaO, thus the decreased the T_m in F1. In addition, the potassium ions lead to an increase in the size of the interstices of the glass network and increase the free volume of the network. Therefore, F1 frites has larger molar volumes than the other frites. This offsets the increase in the atomic weight and causes a decrease in the density of the frit.

In addition, the low temperature melting points (also crystallization temperatures) of fine-ZnO bearing system (N type) could be related to the pronounced physical interactions of ZnO with the silicate chains. The fine-ZnO particles pass lower elastic modulus in comparison with the silicate neat, which caused to arresting of the degradation of silicate chains at lower temperatures through the decreasing of ZnO powder size in frit batch .

On the other hand, by increasing the S ratio the Tg values were increased (ΔTg=154ºC) but the crystallization temperatures were almost unchanged or few increased (ΔTp=17ºC). The increased of Tg values corresponded to the decreased NBO (None Bridging Oxygen) amounts and rigid glass network.

The fine grade frites show 30% higher GFA(glass forming ability), the stability increases up to 4.7% in the fine grade bearing sample (N1) as well, thus it can be said that the fine grade melt has a high viscosity between Tg and T_m typically exhibits a high GFA with a low required cooling rate. The slope and trend of GFA values (Tp- Tg/Tm) in fine ZnO grade bearing frites are sharper than coarse grade ones.The increased stability factor from 0.60(F3) to 0.64(F1) expected from the decrease of elastic moduli. . However, due to the little differences between the glass stability of F and N samples their firing temperatures were not different sufficiently. F3 sample has higher sintering and crystallization temperature compared to the F1 and F2 glazes but because of the K_2O the CTE of the glazes were high. the CTE of the glazes (6.9×10^{-6}/K -6.2×10^{-6}/K) are lower than the CTE of the body (7.4×10^{-6}/K to 9.9×10^{-6}/K) when the compressive stress (due to the unsuitable heating time and temperature) exceeds the strength of glaze, the tile-glaze system will be warped. It was seen in some of the sintered samples.

The Si-O bending vibration (around 800 cm^{-1}) decreases in F1 and F2 frites. The observed low frequency band at 466 cm^{-1} in all the frites samples (F1, F2, N1, N2) was due to vibration of Zn^{2+} metal cations [24]. The zinc ions have the mixed oxygen coordination numbers of four and five; the interconnections between SiO_4 and ZnO are diverse. Either zinc can exist as a network former (tetrahedral coordination) which forms discrete ZnO tetrahedral or as a network modifier (octahedral co-ordination) which breaks up the amorphous silica structure [27-25]. The shift of IR reflection that is related to ZnO in the case of N3 and F3 sample toward the higher wave number could be related to the tetrahedral coordination of ZnO in these systems [26]. The weak band located at 566.82 cm^{-1} ascribed to the symmetric stretching vibrations of the ZnO_4 groups in F2 ,F1 samples as well.

By comparing the N1,N2 samples with the F1,F2 sample's transmittance bands at 780-800 cm^{-1} the shift of the peaks to lower transmittance band in the case of N samples occurred, it can be deduced that the ZnO_3 units were formed instead of ZnO_4 units in N samples [17]. By using nano size ZnO perhaps (in N1,N2) the melt layer at low temperature forms and the Si-O-Zn bonds could not be arranged well which confirmed by FT-IR results

At the temperature above 1000◦C several processes occurred simultaneously including disintegration of wollastonite phase as well as the crystallization of the Willemite and Calcium Aluminum Silicate phases in the F2, N2 and F1,N3 samples respectively. The formation of Willemite phase requires both Zn and Si

cations to interact with each other. The probability and feasibility of such mobility and the interaction would be higher and the diffusion might occurred in a liquid phase of F2 phase.

The F3 glaze has the highest hardness value that can be related to the Anorthite phase with 6 Mohs hardness [27]. The higher relative mole fraction of divalent cations in the residual glass phase of F3 and N3 samples compared to the F2 and N2 ones could be caused to the higher hardness as well. In the F1 and N1 glazes, high percentage of amorphous phase (XRD result) and Wollastonite (with 4.4 Mohs hardness) phase led to the low hardness value.

Both F3 and N3 glazes have the lower gloss values in comparison to the F1 sample. In fact, the effective formation of crystalline phases in these glazes (Anorthite and Wollastonite) declines their surface smoothness and conducts their appearance to the white matte status. The F2 sample has the Willemite phase but perhaps the Anorthite phase formation degraded the gloss value of this system.

The K_2O evaporation from the surface of glazes results in Wollastonite transformation to Parawollastonite. In F3 and N3 samples the K2O wt.% is lower and could cause to the phases differences.

Conclusion

In this study, the frites in SiO_2, Al_2O_3, B_2O_3, ZnO, K_2O, CaO compositions were studied. The $S=K_2O/$ CaO+ ZnO ratios were 0.37(F1), 0.31(F2), 0.24(F3) in the frites batches

It was shown that, Zinc (ZnO) size has the main role in the melting point of wall tile's glazes. The molar volumes of the fine grade ZnO frites are higher than the others.

According to DTA characteristic temperatures, the fine grade ZnO in the frits composition usually increases the glass-forming ability compared to the sample with micronized size ZnO. The onset of the glass's transition point will be boarded, in the case of fine bearing samples.

The fine-bearing sample is more stable than the micronized containing sample.. Also by comparing the glass stability of fine and coarse bearing ZnO frites it can be say that in the F1, the stability increases up to 4.7% compared to N1.

The particle size distribution has also an effect on the crystalline phases of glazes on the Tile surface. The fine grade ZnO containing glazes (N samples) have almost Wollastonite phase as the dominate phase.

The XRD patterns revealed that at the $K_2O/ZnO+CaO$ =0.31 ratio the Willemite phase ($ZnSi_2O_6$) beside Anorthite phase was crystallized in the commercial ZnO containing glazes.

According to FT-IR spectrums by using the nano size ZnO (synthetic powder) perhaps the melt layer at the low temperature forms and the Si-O-Zn bonds could not be arranged well which confirmed by XRD as

well.

Declarations

ACKNOWLEDGMENTS

The authors gratefully acknowledge the financial support of M.S Project, from The Materials and Energy Research Center.

References

1. Demir M, Memesa M, Castignolles P, Wegner G (2006) PMMA/zinc oxide nanocomposites prepared by in-situ bulk polymerization. Macromol Rapid Commun 27:763–770. https://doi.org/10.1002/marc.200500870 No. 10) .
2. Haidong Y, Zhang Z, Han M, Hao X, Zhu F (2005) A general low-temperature route for large-scale fabrication of highly oriented ZnO nanorod/nanotube arrays. J Am Chem Soc 127:2378–2379. https://doi.org/10.1021/ja043121y No. 8) .
3. Rudkovskaya NV, Mikhailenko NY, Decorative zinc-containing crystalline glazes for ornamental ceramics (a review), Glass and ceramics, 58, No. 11–12 (2001) 387–390. https://doi.org/10.1023/A:1014958309094
4. Melchiades G, Rego BT, Higa MSilviaM, Helton J, Boschi AO (2010) Factors affecting glaze transparency of ceramic tiles manufactured by the single firing technique. J Eur Ceram Soc 30(12):2443–2449. https://doi.org/10.1016/j.jeurceramsoc.2010.04.030
5. Pascual JA, Villanueva JU, Villalba AMQ, Transparent tile glaze, Patent US (2006), No. 7,037,868
6. Partyka J, Leś niak M (2016) Preparation of glass –ceramic glazes in the $SiO_2 – Al_2O_3 – CaO – MgO – K_2O – Na_2O – ZnO$ system by variable content of ZnO. Ceram Int 42:8513–8524. https://doi.org/10.1016/j.ceramint.2016.02.077
7. Oytaç ZE, Atan E, Kara A," Use of a Sustainable ZnO in Place of Standard ZnO in Mustafa Fahri Özer "Ceramic Research Center INC, Anadolu University – Türkiye Ceramic Tile Production, IMMC 2016,18th International Metallurgy & Materials Congress,197–203
8. Casasola R, Rincón JM, Romero M (2012) Glass-ceramic glazes for ceramic tiles – a review. Journal of Materials Science 47:553–582. https://doi.org/10.1007/s10853-011-5981-y
9. Mehdikhani B, Borhani GH (2013) Optical spectroscopy of sodium silicate glasses prepared with nano- and micro-sized iron oxide particles. Processing Application of Ceramics 7(3):117–121. https://doi.org/10.2298/PAC1303117M
10. Diaz PM, Palanikumar K, Kumar PR, "Effect of addition of nano zirconia in ceramic glazes" Adv Mater Res, 984–985 (2014) 488–494. https://doi.org/10.4028/www.scientific.net/AMR.984-985.488
11. Shaohua W, Peng C, Lü M, Wu J (2013) Effect of ZnO on crystallization of zircon from zirconium-based glaze. J Am Ceram Soc 96:2054–2057. https://doi.org/10.1111/jace.12441 No. 7) .

12. Sheckler AC, Dinge RD, Effect of Particle Size Distribution on the Melting of Soda-lime-Silica Glass, Journal of the American Ceramic Society 73 NoI (1990)24–30. https://doi.org/10.1111/j.1151-2916.1990.tb05084.x
13. Bernardin A, Michael A (2009) The influence of particle size distribution on the surface appearance of glazed tiles. Dyes Pigm 80(1):121–124
14. https://doi.org/10.1016/j.dyepig.2008.05.011
15. Melchiades FG, Neto CL, Alves HJ, Boschi AO, Formulação de Fritas Cerâmicas com Auxílio da Técnica dePlanejamento Estatístico de Experimentos,Cerâmica Industrial, 14, No.3 (2009) 23–29
16. Seo BH, Kim H, Suh DH (2009) Effects of alkali and alkaline-earth oxides on thermal, dielectrical, and optical properties of zinc borate glasses for transparent dielectric". Met Mater Int 15:983–987. https://doi.org/10.1007/s12540-009-0983-x
17. Chanshetti UB, Shelke VA, Jadhav SM, Shankarwar SG, Chondhekar TK, Shankarwar AG, Sudarsan V, Jogad MS, Density and molar volume studies of phosphate glasses, Facta universitatis-series: Physics, Chemistry and Technology, 9, No. 1 (2011) 29–36. https://doi.org/10.2298/FUPCT1101029C
18. Ana KP, Šesták J (2012) Forty years of the Hrubý glass-forming coefficient via DTA when comparing other criteria in relation to the glass stability and vitrification ability. J Therm Anal Calorim 110(2):997–1004. https://doi.org/10.1007/s10973-011-1926-6
19. Zanotto ED, Isothermal and adiabatic nucleation in glass, Journal of non-crystalline solids, 89, No. 3 (1987) 361–370. https://doi.org/10.1016/S0022-3093(87)80278-8
20. Zanotto ED, James PF (1985) "Experimental tests of the classical nucleation theory for glasses. J Non-Cryst Solids 74:No. 2–3. https://doi.org/10.1016/0022-3093(85)90080-8 373–394.
21. Cabral AA, Fokin VM, Zanotto ED (2010) On the determination of nucleation rates in glasses by nonisothermal methods. J Am Ceram Soc 93:2438–2440. https://doi.org/10.1111/j.1551-2916.2010.03782.x No. 9)
22. Xiang Y, Jincheng D, Lawrie D (2013) Structure and diffusion of ZnO–SrO–CaO–Na_2O–SiO_2 bioactive glasses: a combined high energy X-ray. RSC Advances 3:5966–5978. https://doi.org/10.1039/C3RA23231J No.17)
23. Ozel E, Turan S (2003) Production and characterisation of iron-chromium pigments and their interactions with transparent glazes. J Eur Ceram Soc 23:2097–2104
24. Sugimura HOhsatoT (1986) Morphology of synthetic β-wollastonite and para-wollastonite. J Cryst Growth 74(3):656–658. https://doi.org/10.1016/0022-0248(86)90212-5
25. Cabral AA, Fokin VM (2010) E.D. Zanotto,On the determination of nucleation rates in glasses by nonisothermal methods. Journal of The American Ceramic Society 93:2438–2440. https://doi.org/10.1111/j.1551-2916.2010.03782.x
26. Rosenthal A (1987) S. H. Garofalini,Structural Role of Zinc Oxide in Silica and Soda-Silica Glasses. Journal of The American Ceramic Society 70:821–826. https://doi.org/10.1111/j.1151-

2916.1987.tb05634.x No.11) .

27. Marinković ZV, St. N.Romčevićb, Spectroscopic study of spinel ZnCr2O4 obtained from mechanically activated ZnO–Cr_2O_3 mixtures, Journal of the European Ceramic Society, 27, No. 2–3(2007) 903–907. https://doi.org/10.1016/j.jeurceramsoc.2006.04.057
28. Kavanova M, Klouzkova A, Klouzek J (2017) Characterization Interaction Between, Glazes and Ceramic bodies. Ceramics-Silikáty 61:267–275. DOI:10.13168/cs.2017.0025

Tables

Table1.The wt. % of used oxides in F1, F2 and F3 systems

frites composition	K_2O	SiO_2	Al_2O_3	B_2O_3	CaO	ZnO	K_2O/ CaO+ ZnO
F1	7.5	60.1	8.2	4.2	12.7	7.1	0.37
F2	6.5	60.1	8.2	4.2	15.2	5.8	0.30
F3	3.5	60.1	8.2	4.2	17.7	4.3	0.24

Table 2 the wt. % of additives used in slurries

The additive	Water	Clay	CMC
Weight percent	40	5	0.5

Table 3 the density and the melting temperatures of three series of the frites

name	S=K_2O/CaO+ZnO	Molar mass(g)	Melting temperature ©	Density (g/cm^3)	Molar Volume	CTE×10^{-6}/K
F1	0.377	249.72	1450	2.54	98.31	6.96
F2	0.31	246.811	1470	2.55	96.78	6.88
F3	0.24	243.52	1550	2.53	96.25	6.28
N1	0.377	249.72	1350	2.56	97.54	-
N2	0.31	246.811	1400	2.58	95.63	-
N3	0.24	243.52	1450	2.55	95.49	-

Table 4. Characteristic DTA' peaks temperatures of frites

T_P-T_g	T_P ºC	T_g ºC	Characteristic temperatures
310	928	618	F1
226	930	704	F2
173	945	772	F3
295	889	594	N1
226	916	690	N2
135	860	725	N3

Table 5 the sintering temperatures and the sintering time of obtained glazes with respect to appearance

Name	Sintering temperatureº©	60 minute	90 minute	150 minute	210 minute
F1	1060	warping	transparent	opaque	Cracked surface
F2	1080	warping	good	Phase separated(p.s)	cracked
F3	1160	warping	good	p.s	p.s
F1	1180		Matt-white	Matt-white	
F2	1180	white	Matt-white	Matt-white	Cracked surface
F3	1180	white	white	white	cracked
N1	1060	Raw glaze	good	-	Cracked surface
N2	1060	Raw glaze	good	-	cracked
N3	1060	warping	good	-	Cracked surface

Table 6 .The micro hardness and crystalline phases of glazes heat treated at 1060ºC for 3 minutes with 90 minutes heating time

name	S	microhardness(Hv)	Crystalline phase
F1	0.377	730±14	Wollastonite
F2	0.31	744±20	Anorthite + Willemite
F3	0.24	817±35	Anorthite
N1	0.377	755±16	Calcium Silicate
N2	0.31	635±-53	Wollastonite+ Willemite
N3	0.24	742±-42	Wollastonite

Table 7 The CIE Lab parameters gloss values of the glazes

Sample	L*	a*	b*	c*	Specular Gloss(GU)
F1	57.51	9.56	-5.95	11.27	86.1
F2	74.41	1.7	0.47	1.77	83.2
F3	76.53	2.33	-0.04	2.33	67.30
N1	65.14	6.74	3.87	7.77	82.3
N2	68.05	5.41	2.64	6.02	84.3
N3	63.12	6.3	4.41	8.1	52.3

Figures

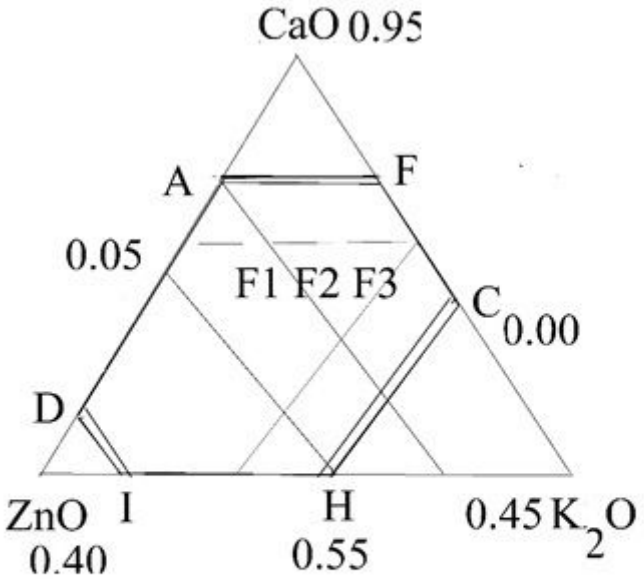

Figure 1

The F1,F2, F3 compositions were selected from the center of compositional triangle proposed by [14]

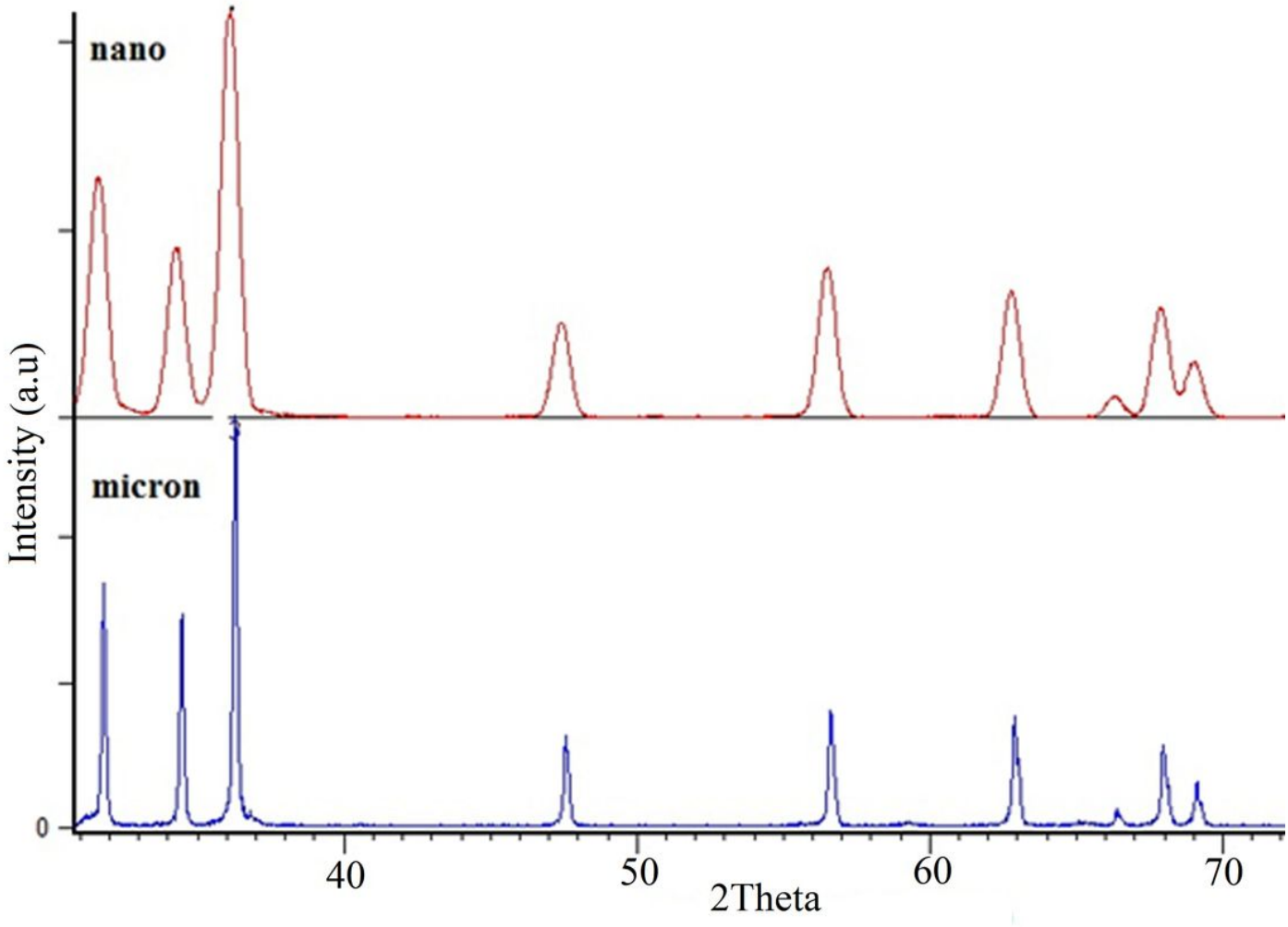

Figure 2

The XRD patterns of the (a) nano –synthesized (b) commercial ZnO

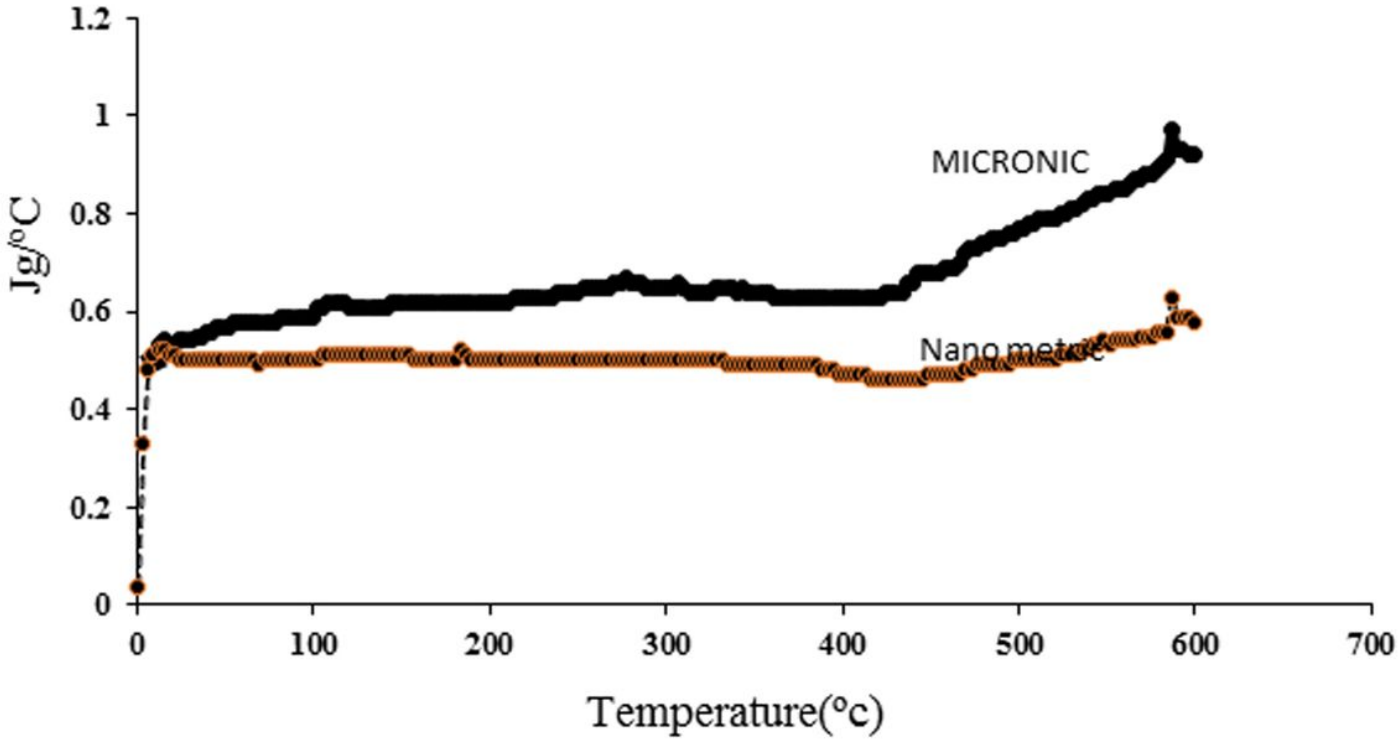

Figure 3

The Cp values of Nano and micro size of used ZnO powder measured by DSC,

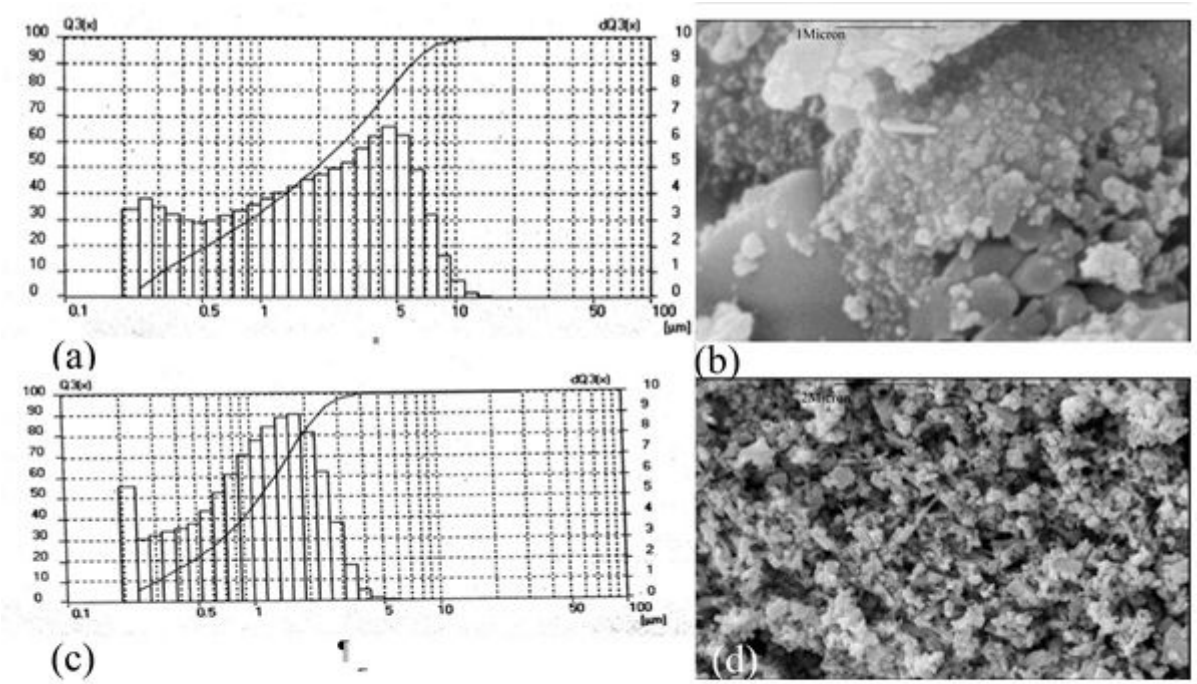

Figure 4

a the commercial ZnO powder particle size analysis b The SEM micrograph of the commercial ZnO powder c the synthesized ZnO powder d The SEM micrograph of the synthesized ZnO powder

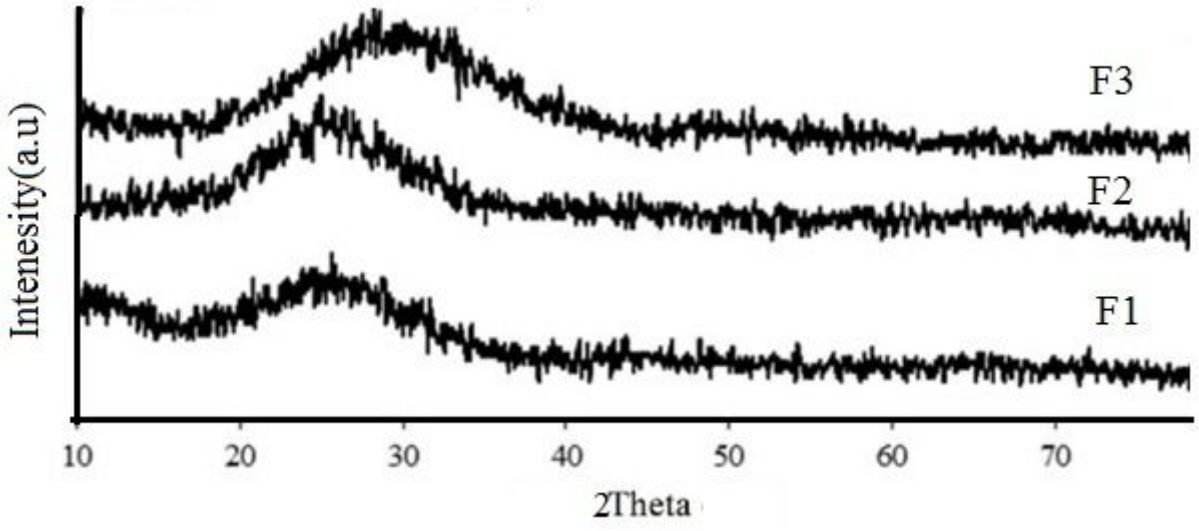

Figure 5

The XRD amorphous pattern of obtained frite F2 and F1

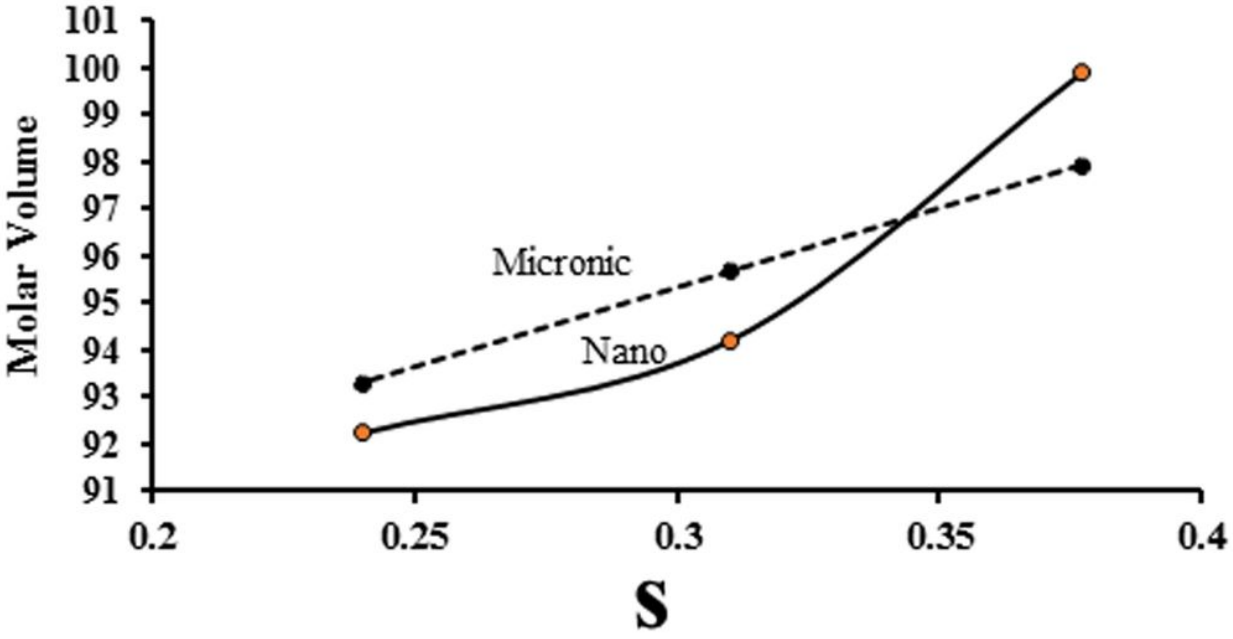

Figure 6

The molar volumes vs. S ratio with respect to ZnO's PSA

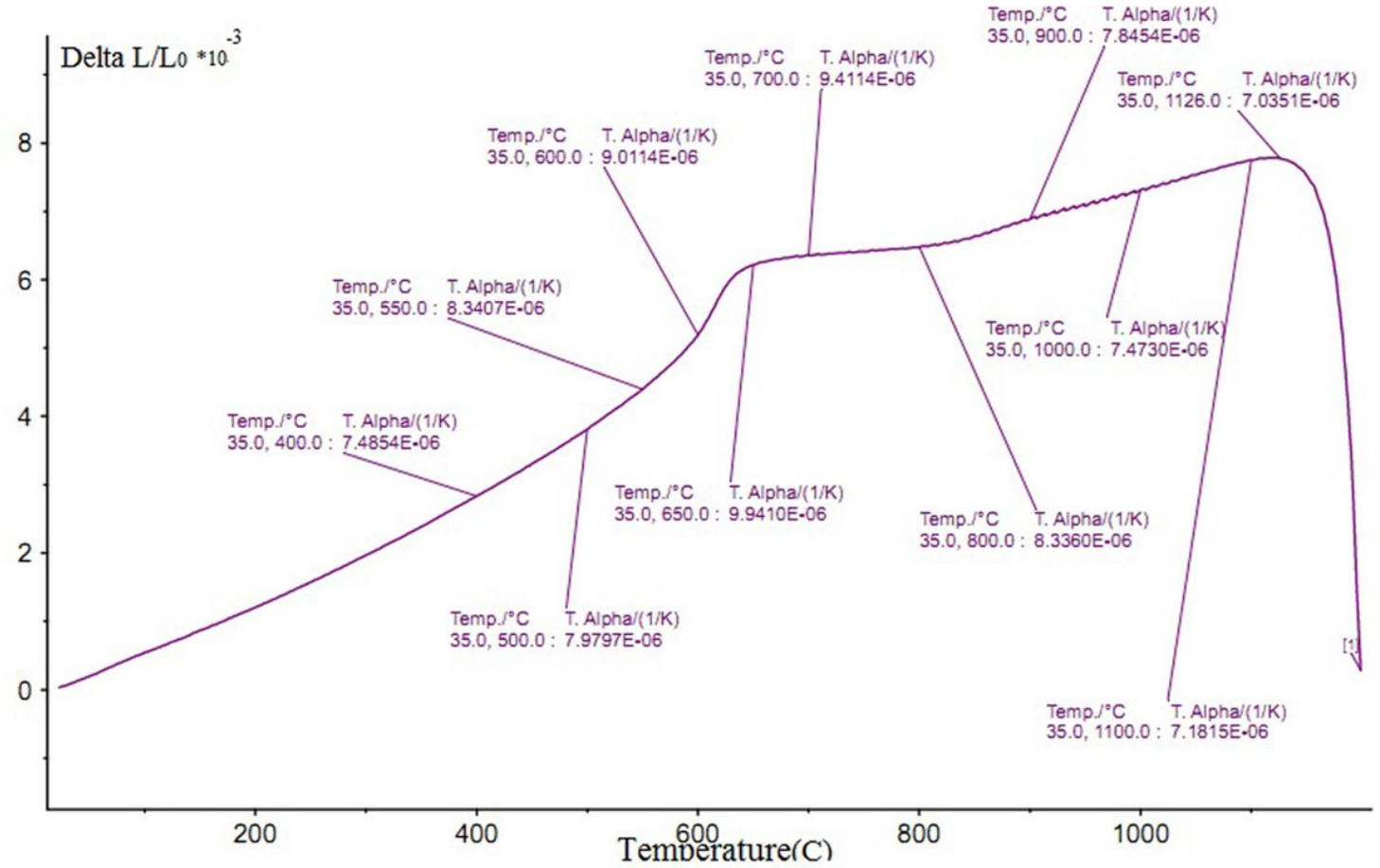

Figure 7

The dilatometer result of tile's body

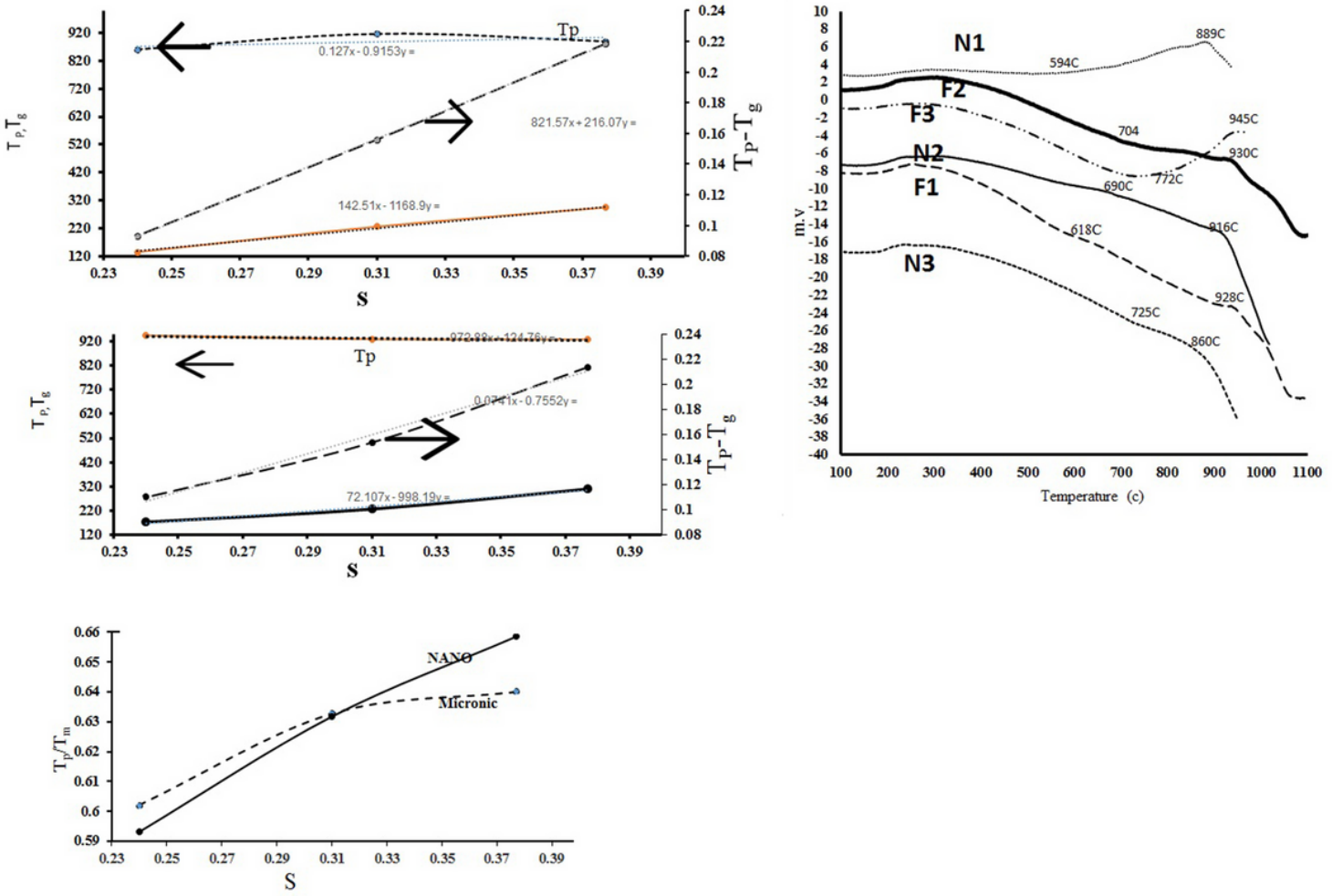

Figure 8

The DTA results of obtained frites by 10ºC/min heating rate a The variation Tp,Tg, Tp-Tg/Tm temperatures by the S ratio in fine grade system b The variation Tp, Tg, Tp-Tg/Tm temperatures by the S ratio in micronic system c The Tg/Tm values vs. glass S ratio in micronic and fine ZnO bearing system d The Tp-Tg/Tm values vs. S ratio in micronic and fine ZnO bearing system

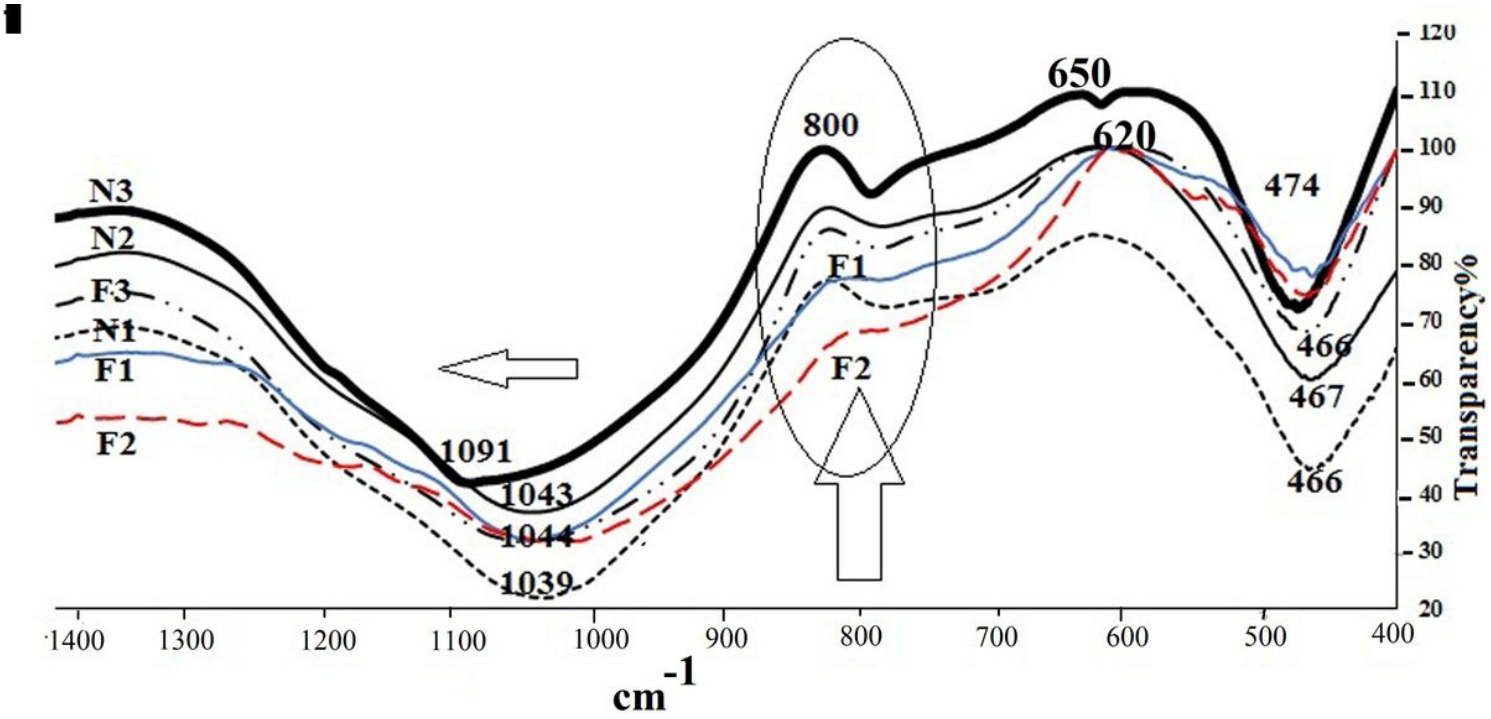

Figure 9

The FT-IR spectrums of F1,F2, F3, N1,N2,N3 glasses , the intensity of bending vibration of F2,F1 at 800 cm -1 are weak

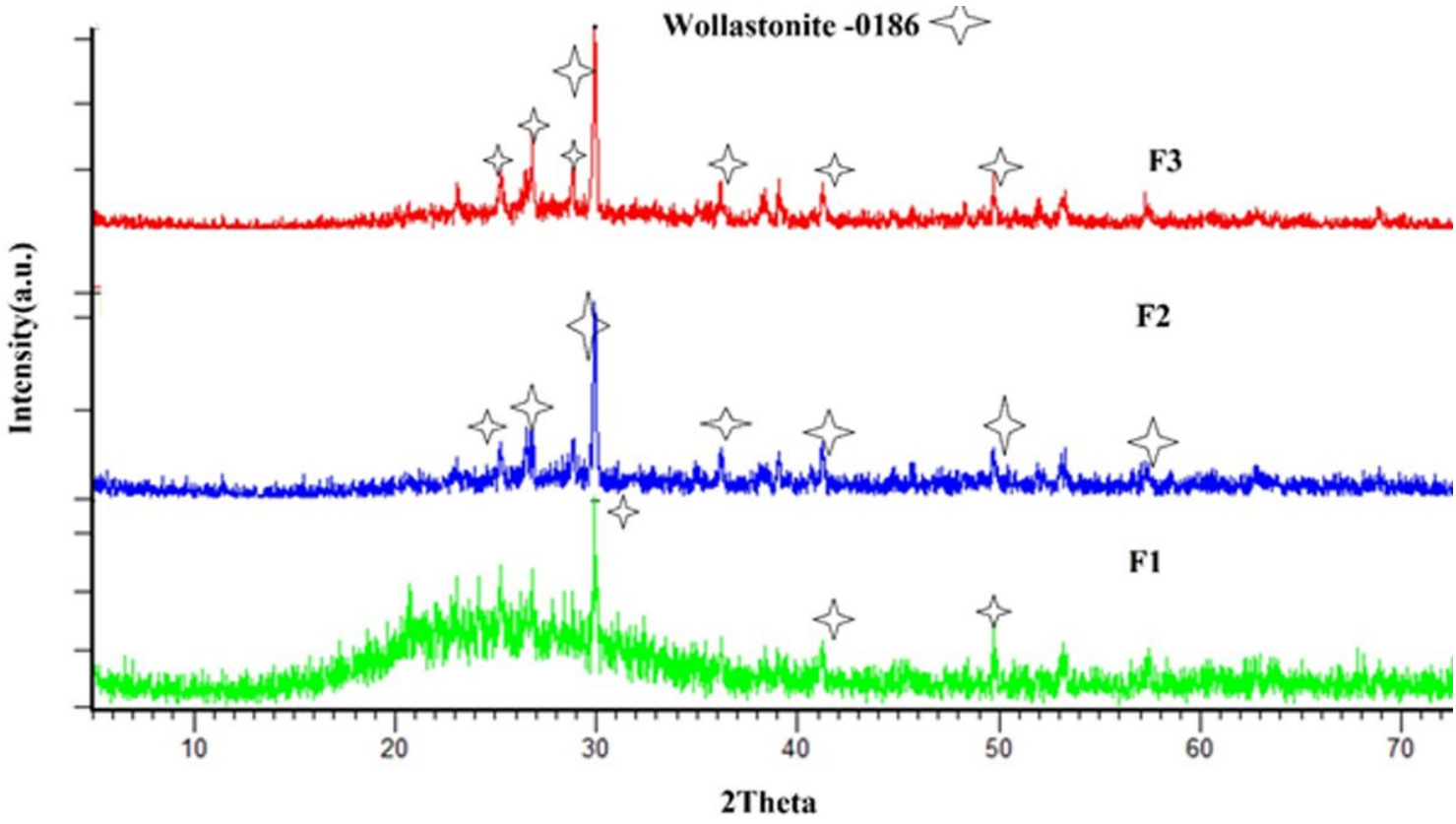

Figure 10

heat treated F2 , F1 and F3 at 1000°C for 30 min. in 90 minutes heating time .

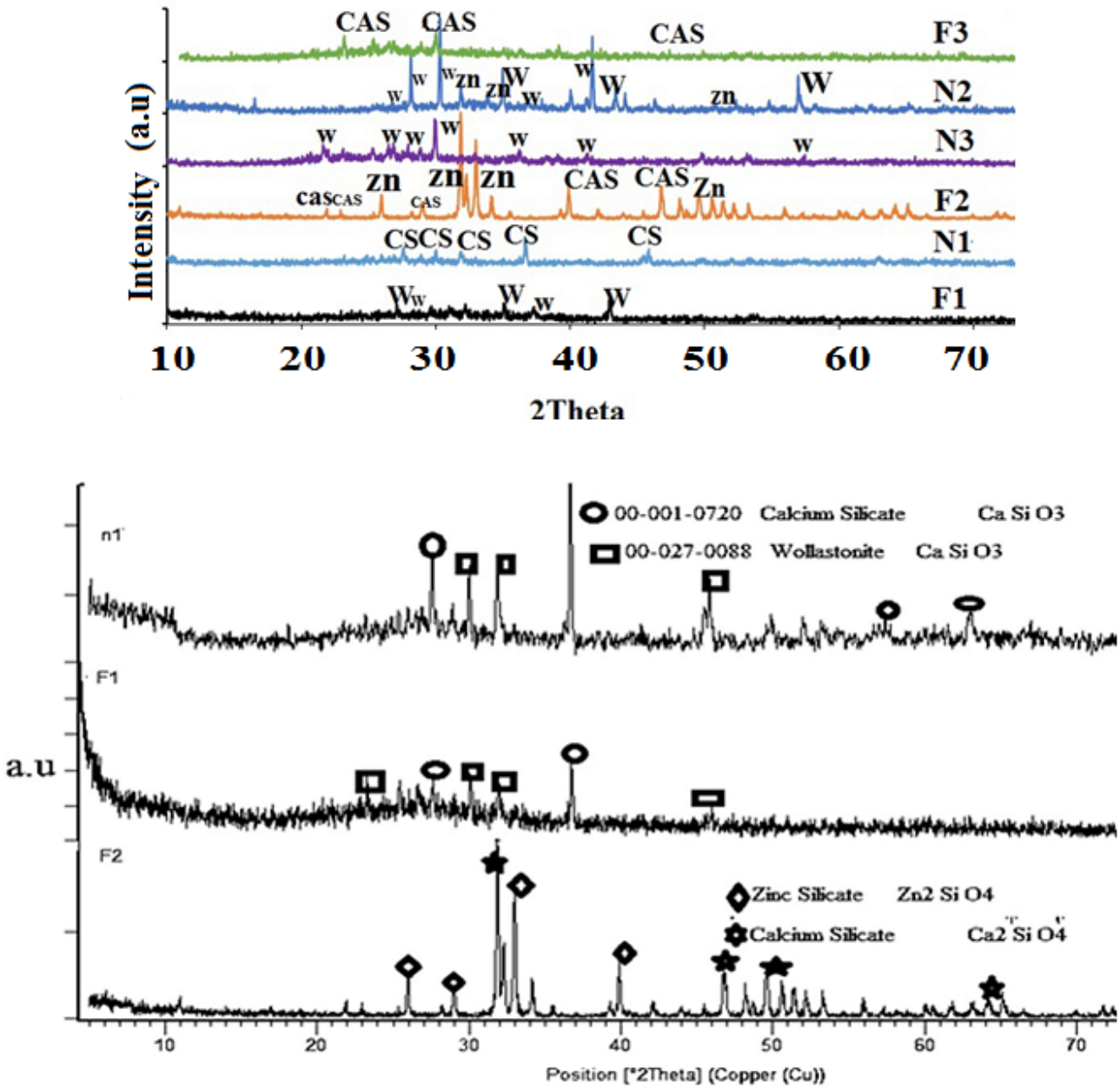

Figure 11

XRD results of heat-treated glazes at 1060°C for 3 min. in 90 minutes heating time.(zn: Willemite (zinc silicate),w: wollastonite, CAS: Calcium Aluminum Silicate,CS: Calcium Silicate)

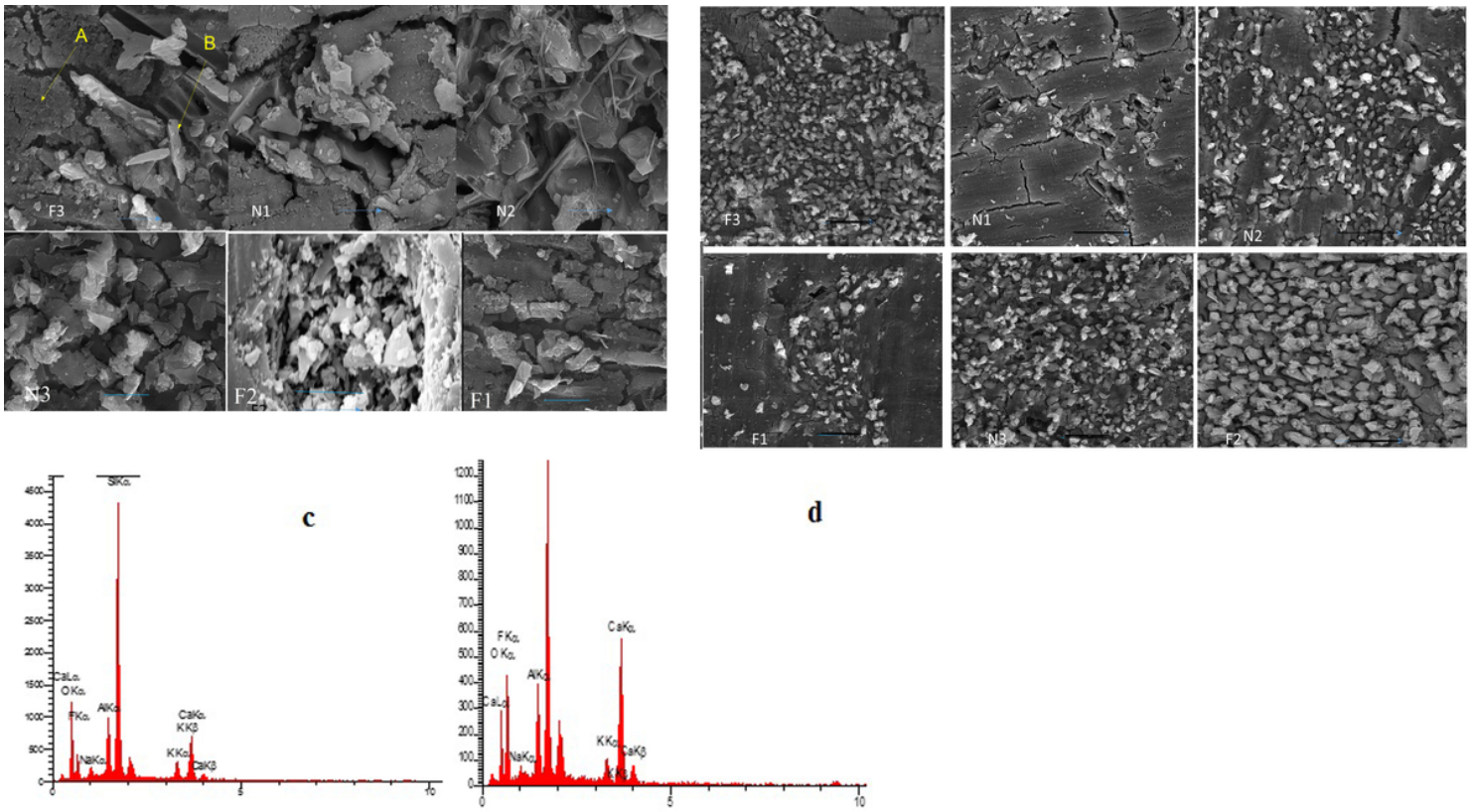

Figure 12

a The SEM micrographs of polished and etched glazes by ×2000magnification (scale bar corresponded to 10μm) b The SEM micrographs of polished and etched glazes by ×10000magnification (scale bar corresponded to 2μm)

Supplementary Files

This is a list of supplementary files associated with this preprint. Click to download.

- Extendedabstract.docx